AIAA Guidance, Navigation, and Control Conference and Exhibit
11-14 August 2003, Austin, Texas

AIAA 2003-5430

ADAPTIVE CONTROL OF A FLEXIBLE MEMBRANE USING ACOUSTIC EXCITATION AND OPTICAL SENSING

Jesse Hoagg *and Dennis Bernstein †‡
Dept. of Aerospace Engineering
University of Michigan
Ann Arbor, MI 48109-2140
dsbaero@umich.edu

Seth L. Lacy §
AFRL/VSSV
3550 Aberdeen Ave. SE
Kirtland AFB, NM 87117

Ravinder Venugopal ¶
Sysendes, Inc.
4-1804, Rue Tupper
Montreal, QC H3H 1N4
Canada
rvenugopal@sysendes.com

ABSTRACT

Flexible membranes are envisioned as a key component of large, lightweight, space-based systems. This paper focuses on the problem of adaptive disturbance rejection, that is, the rejection of external disturbances with unknown spectral content. It describes the design and operation of a laboratory testbed involving a flexible membrane with acoustic excitation and optical sensing. The ARMARKOV adaptive disturbance rejection algorithm is used to reject single- and dual-tone disturbances without knowledge of the disturbance spectrum and with limited modeling of the membrane dynamics.

INTRODUCTION

Flexible membranes are envisioned as a key component of space-based optical systems. In particular, large optical apertures are desirable for a wide range of missions such as laser beam projection and optical imaging. For such missions the optical accuracy of membranes is a significant engineering challenge.[1,2] An alternative to the use of large monolithic membranes is sparse aperture technology.[3] This approach allows compact packaging and the use of rigid mirrors. Nevertheless, because of weight and volume launch restrictions, deployable, ultra-lightweight membranes are an enabling technology for missions requiring large apertures.

To realize these objectives, researchers have developed membrane material with optical tolerances.[4,5] In addition, wavefront correction techniques based on phase-modulated liquid crystals have been developed for sub-wavelength compensation.[6]

Large membrane mirrors will be deployed from a stowed configuration, and thus initial deployment errors are expected to require active compensation on the order of multiple wavelengths. It is useful to distinguish between active compensation for shape control and active compensation for disturbance rejection. Each type of compensation entails distinct requirements and challenges.

For shape control the objective is to establish an equilibrium shape that is different from the (imperfect) uncontrolled shape. To do this, the actuators must have sufficient spatial input to achieve and hold the desired shape, which in most applications is either flat or parabolic. Prestressing and preshaping are thus of interest.[7]

For disturbance rejection the objective is to maintain the given uncontrolled shape against disturbances. Assuming that controllability and observability requirements are met by avoiding modal nodes, a small number of sensors and actuators has the ability to maintain the equilibrium shape at least at a finite number of points. To do this, the sensors and actuators must have sufficient bandwidth, although the achievable performance is limited by their spatial arrangement.[8]

Although shape control does not place a bandwidth requirement on the sensors and actuators, the ability to establish a desired equilibrium shape places a requirement on the number and placement of actuators. Technologically, this requirement may be more severe than the sensor/actuator require-

*Graduate Student
†Professor
‡This research was supported in part by the Air Force Office of Scientific Research under grant F49620—01–1–0094.
§Research Aerospace Engineer, Member AIAA
¶Founder and Senior Consulting Engineer

Copyright © 2003 by the American Institute of Aeronautics and Astronautics, Inc. All rights reserved.

ments for disturbance rejection. In fact, a single actuator may be able to suppress vibration at a large number of points, while many actuators may be needed to achieve a desired shape.

The development of effective membrane actuators for shape and disturbance requirements is a nontrivial engineering task. Several actuation mechanisms have been investigated, including electrostatic,[9,10] electron gun,[11] and boundary actuation[12] techniques. With magnetically permeable membrane material, electromagnetic actuation is also possible as is actuation based on fluid pressure.

For electrostatic and electromagnetic actuation, the actuation forces satisfy an inverse square law in terms of the actuation gap. This input nonlinearity requires special treatment to avoid the snap-through instability that occurs at less than one-third of the initial gap.[13–15]

In the present paper we describe the development of an experimental testbed based on a flexible membrane. This testbed was designed for implementing adaptive control laws for disturbance rejection. Hence shape control objectives are not considered. Instead, this testbed is designed to focus on the challenges that arise in rejecting external disturbances with unknown spectrum and with uncertainty in the membrane dynamics.

For adaptive disturbance rejection we apply the ARMARKOV adaptive disturbance rejection algorithm.[16–18] This algorithm is an adaptive feedback control law that does not require direct measurements of the system disturbance and permits arbitrary spatial arrangements of the sensors and actuators. In addition, the algorithm is effective in the presence of single-, multi-tone, and broadband disturbances, and it requires only limited modeling of the plant dynamics.

In Section 2 we describe the membrane testbed including the choice of sensors and actuators. In Section 3 we state the standard disturbance rejection problem, and in Sections 4 we review the ARMARKOV adaptive disturbance rejection algorithm. The experimental implementation is described in Section 5. Finally, we draw some conclusions in Section 6.

EXPERIMENTAL TESTBED DESCRIPTION

The membrane testbed involves four main components, namely, the membrane itself, the disturbance source, the control actuation, and the measurement sensing.

The membrane is a circular, plastic drumhead, model number LW4240, that measures 40 inches in diameter and is mounted on a bass drum. The drumhead, U.S. patent number 2,979,981, and bass drum were manufactured in Monroe, NC, by Ludwig Drums, a division of the Selmer Company, Inc.

Figure 1 shows the frequency response of the membrane to a band-limited Gaussian white noise disturbance. This frequency response data indicate that the drumhead does not behave according to the classical mathematical model for a membrane.[19] In particular, the modal frequencies are higher than predicted by the classical membrane model due to drumhead stiffness, which is not accounted for in the classical model. Similarly, the drumhead cannot be modeled as a thin plate. Figure 2 compares the experimental modal frequencies of the drumhead with the model frequencies predicted by the classic membrane model and the thin plate model. An accurate model for drumhead behavior would require a membrane-like model incorporating stiffness.

Membrane disturbance is achieved acoustically by a single 6.5-inch speaker suspended approximately 6 inches above the membrane suface. The disturbance speaker is a model Competition 6.5C, manufactured by Kicker USA, a division of Stillwater Designs and Audio, Inc., Stillwater, OK. Figure 3 shows the membrane testbed including the disturbance actuator.

Acoustic control actuation is provided by a circular arrangement of seven 12-inch speakers, model Kappa Perfect 12.1, manufactured by Infinity System, Inc., China. The speaker array is shown in Figure 4. The speakers are driven by four model CE 1000 amplifiers, manufactured by Crown Audio, Inc., Elkhart, IN. The amplifiers provide eight amplification channels each with 275 watts of power at 8 ohms resistance.

For feedback control sensing is provided by optical means. Specifically, a 1-mW laser is reflected directly off of the membrane, without the aid of a mounted mirror, and is sensed by a 2-cm diameter optical sensor. Figure 3 shows both the laser and optical sensor. The optical sensor, model OT-301,

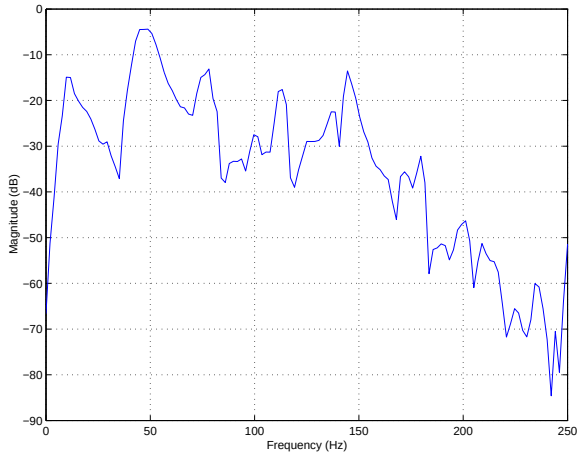

Figure 1: Frequency response of the membrane to a Gaussian white noise disturbance from a control actuator. The model frequencies show that the membrane possesses stiffness.

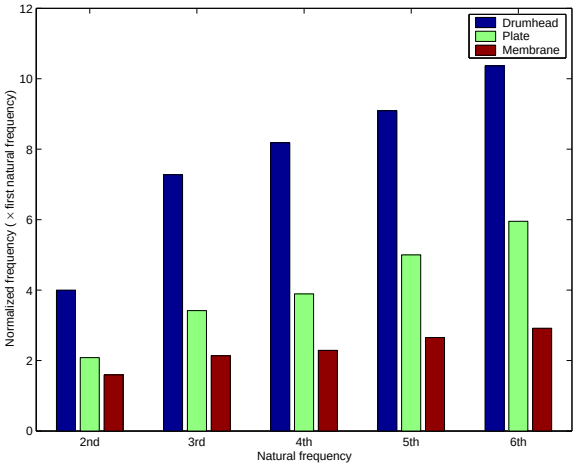

Figure 2: Natural frequencies for the drumhead compared to the thin plate and membrane model predictions. The normalized natural frequencies show that the drumhead is neither a plate nor a membrane.

is manufactured by On-Track Photonics, Inc., Lake Forest, CA. This sensor provides 2-axis measurements which are sensitive to deflections of the beam along independent directions. Hence the optical sensor effectively measures membrane slope rather than vertical displacement.

ARMARKOV MODELING

Consider the linear discrete-time two vector-input, two vector-output (TITO) system shown in Figure 5. The *disturbance* $w(k)$, the *control* $u(k)$, the *measurement* $y(k)$ and the *performance* $z(k)$ are in $\mathcal{R}^{m_w}, \mathcal{R}^{m_u}, \mathcal{R}^{l_y}$ and $\mathcal{R}^{l_z}$, respectively. The system can be written in state space form as

$$x(k+1) = Ax(k) + Bu(k) + D_1 w(k), \quad (1)$$
$$z(k) = E_1 x(k) + E_2 u(k) + E_0 w(k), \quad (2)$$
$$y(k) = Cx(k) + Du(k) + D_2 w(k), \quad (3)$$

or equivalently in terms of transfer matrices

$$z = G_{zw} w + G_{zu} u, \quad (4)$$
$$y = G_{yw} w + G_{yu} u. \quad (5)$$

The controller G_c generates the control signal $u(k)$ based on the measurement $y(k)$, that is,

$$u = G_c y. \quad (6)$$

The objective of the standard problem is to determine a controller G_c that produces a control signal

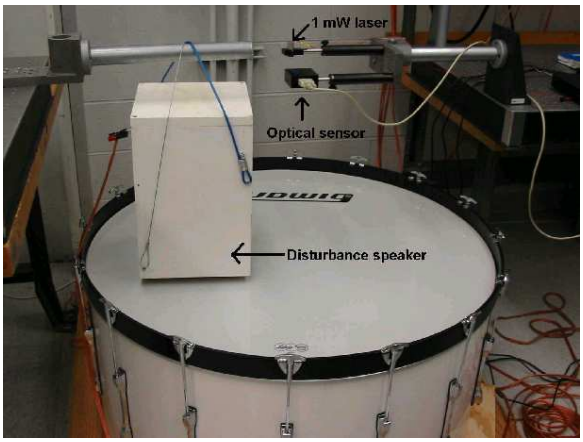

Figure 3: Membrane control testbed. The acoustic disturbance is provided by a 6.5-inch speaker. Feedback sensing is accomplished through a 1-mW laser and a 2-axis optical sensor.

Figure 4: Control actuator configuration. The 7-speaker arrangement provides acoustic actuation of the membrane displacement.

$u(k)$ based on the measurement $y(k)$ such that a performance measure involving $z(k)$ is minimized.

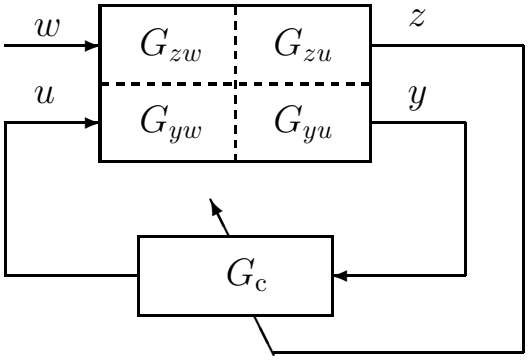

Figure 5: The ARMARKOV adaptive control architecture involves an instantaneously (frozen-time) linear feedback controller adapted by using measurements of the performance z.

We now review the ARMARKOV/Toeplitz[16,20] model of (1)-(3). Defining the Markov parameters of the system by

$$H_{yu,-1} \triangleq D, \quad H_{yu,j} \triangleq CA^jB, \quad j \geq 0, \tag{7}$$

$$H_{yw,-1} \triangleq D_2, \quad H_{yw,j} \triangleq CA^jD_1, \quad j \geq 0, \tag{8}$$

$$H_{zu,-1} \triangleq E_2, \quad H_{zu,j} \triangleq E_1A^jB, \quad j \geq 0, \tag{9}$$

$$H_{zw,-1} \triangleq E_0, \quad H_{zw,j} \triangleq E_1A^jD_1, \quad j \geq 0, \tag{10}$$

the ARMARKOV model of (1)-(3) with μ Markov parameters is given by

$$\begin{aligned} z(k) &= \sum_{j=1}^{n} -\alpha_j z(k-\mu-j+1) \\ &+ \sum_{j=1}^{\mu} H_{zw,j-2} w(k-j+1) \\ &+ \sum_{j=1}^{n} \mathcal{B}_{zw,j} w(k-\mu-j+1) \\ &+ \sum_{j=1}^{\mu} H_{zu,j-2} u(k-j+1) \\ &+ \sum_{j=1}^{n} \mathcal{B}_{zu,j} u(k-\mu-j+1), \end{aligned} \tag{11}$$

$$\begin{aligned} y(k) &= \sum_{j=1}^{n} -\alpha_j y(k-\mu-j+1) \\ &+ \sum_{j=1}^{\mu} H_{yw,j-2} w(k-j+1) \\ &+ \sum_{j=1}^{n} \mathcal{B}_{yw,j} w(k-\mu-j+1) \\ &+ \sum_{j=1}^{\mu} H_{yu,j-2} u(k-j+1) \\ &+ \sum_{j=1}^{n} \mathcal{B}_{yu,j} u(k-\mu-j+1), \end{aligned} \tag{12}$$

where $\alpha_j \in \mathcal{R}$, $\mathcal{B}_{zw,j}, H_{zw,j} \in \mathcal{R}^{l_z \times m_w}$, $\mathcal{B}_{zu,j}, H_{zu,j} \in \mathcal{R}^{l_z \times m_u}$, $\mathcal{B}_{yw,j}, H_{yw,j} \in \mathcal{R}^{l_y \times m_w}$ and $\mathcal{B}_{yu,j}, H_{yu,j} \in \mathcal{R}^{l_y \times m_u}$.

Next, define the *extended performance vector* $Z(k)$, the *extended measurement vector* $Y(k)$ and the *extended control vector* $U(k)$ by

$$Z(k) \triangleq \begin{bmatrix} z(k) & \cdots & z(k-p+1) \end{bmatrix}^{\mathrm{T}}, \tag{13}$$

$$Y(k) \triangleq \begin{bmatrix} y(k) & \cdots & y(k-p+1) \end{bmatrix}^{\mathrm{T}}, \tag{14}$$

$$U(k) \triangleq \begin{bmatrix} u(k) & \cdots & u(k-p_{\mathrm{c}}+1) \end{bmatrix}^{\mathrm{T}}, \tag{15}$$

where p is a positive integer and $p_{\mathrm{c}} \triangleq \mu+n+p-1$, and the *ARMARKOV regressor vectors* $\Phi_{zw}(k)$ and $\Phi_{yw}(k)$ by

$$\begin{aligned} \Phi_{zw}(k) \triangleq \big[& z(k-\mu) \cdots z(k-\mu-p-n+2) \\ & w(k) \cdots w(k-\mu-p-n+2) \big]^{\mathrm{T}}, \end{aligned} \tag{16}$$

$$\begin{aligned} \Phi_{yw}(k) \triangleq \big[& y(k-\mu) \cdots y(k-\mu-p-n+2) \\ & w(k) \cdots w(k-\mu-p-n+2) \big]^{\mathrm{T}}. \end{aligned} \tag{17}$$

Then (11) and (12) can be written as an ARMARKOV/Toeplitz model in the form

$$Z(k) = W_{zw}\Phi_{zw}(k) + B_{zu}U(k), \quad (18)$$
$$Y(k) = W_{yw}\Phi_{yw}(k) + B_{yu}U(k), \quad (19)$$

where the block-Toeplitz matrices W_{zw}, B_{zu}, W_{yw} and B_{yu} contain the parameters α_j, $\mathcal{B}_{zw,j}$, $H_{zw,j}$, $\mathcal{B}_{zu,j}$, $H_{zu,j}$, $\mathcal{B}_{yw,j}$, $H_{yw,j}$, $\mathcal{B}_{yu,j}$ and $H_{yu,j}$. These matrices are as defined in.[16]

ADAPTIVE DISTURBANCE REJECTION

In this section we review the ARMARKOV adaptive disturbance rejection feedback algorithm for the TITO system represented by (18) and (19).[16] We use a strictly proper controller in ARMARKOV form of order n_c with μ_c Markov parameters, so that the control $u(k)$ is given by

$$\begin{aligned} u(k) &= \sum_{j=1}^{n_c} -\alpha_{c,j}(k)u(k-\mu_c-j+1) \\ &+ \sum_{j=1}^{\mu_c-1} H_{c,j-1}(k)y(k-j+1) \\ &+ \sum_{j=1}^{n_c} \mathcal{B}_{c,j}(k)y(k-\mu_c-j+1), \end{aligned} \quad (20)$$

where $H_{c,j} \in \mathcal{R}^{m_u \times l_y}$ are the Markov parameters of the controller. Next, define the *controller parameter block vector*

$$\theta(k) \triangleq \begin{bmatrix} -\alpha_{c,1}(k)I_{m_u} & \cdots & -\alpha_{c,n_c}(k)I_{m_u} \\ H_{c,0}(k) & \cdots & H_{c,\mu_c-2}(k) \\ \mathcal{B}_{c,1}(k) & \cdots & \mathcal{B}_{c,n_c}(k) \end{bmatrix}. \quad (21)$$

Now from (15) and (21) it follows that $U(k)$ is given by

$$U(k) = \sum_{i=1}^{p_c} L_i\theta(k-i+1)R_i\Phi_{uy}(k), \quad (22)$$

and the control input to the system $u(k)$ at the instant k is given by

$$u(k) = \theta(k)R_1\Phi_{uy}(k), \quad (23)$$

with

$$\Phi_{uy}(k) \triangleq \begin{bmatrix} u(k-\mu_c) & \cdots & u(k-\mu_c-n_c-p_c+2) \\ y(k-1) & \cdots & y(k-\mu_c-n_c-p_c+2) \end{bmatrix}^{\mathrm{T}},$$

and where L_i and R_i are constraint matrices that maintain the block-Toeplitz structure of the control weight matrix in (22).[16] Thus, from (18) and (22) we obtain

$$\begin{aligned} Z(k) &= W_{zw}\Phi_{zw}(k) \\ &+ B_{zu}\sum_{i=1}^{p_c} L_i\theta(k-i+1)R_i\Phi_{uy}(k). \end{aligned} \quad (24)$$

Next, we define a cost function that evaluates the performance of the current value of $\theta(k)$ based upon the behavior of the system during the previous p_c steps. Therefore, we define the *estimated performance* $\hat{Z}(k)$ by

$$\begin{aligned} \hat{Z}(k) &\triangleq W_{zw}\Phi_{zw}(k) \\ &+ B_{zu}\sum_{i=1}^{p_c} L_i\theta(k)R_i\Phi_{uy}(k), \end{aligned} \quad (25)$$

which has the same form as (24) but with $\theta(k-i+1)$ replaced by the current parameter block vector $\theta(k)$. Using (25) we define the *estimated performance cost function*

$$J(k) = \frac{1}{2}\hat{Z}^{\mathrm{T}}(k)\hat{Z}(k). \quad (26)$$

The gradient of $J(k)$ with respect to $\theta(k)$ is given by

$$\frac{\partial J(k)}{\partial \theta(k)} = \sum_{i=1}^{p_c} L_i^{\mathrm{T}}B_{zu}^{\mathrm{T}}\hat{Z}(k)\Phi_{uy}^{\mathrm{T}}(k)R_i^{\mathrm{T}}. \quad (27)$$

Note that $\hat{Z}(k)$ cannot be evaluated using (25) since $w(k)$ is not available and thus $\Phi_{zw}(k)$ is unknown. However, it follows from (18) and (25) that

$$\hat{Z}(k) = Z(k) - B_{zu}\left(U(k) - \sum_{i=1}^{p_c} L_i\theta(k)R_i\Phi_{uy}(k)\right),$$

which can be used to evaluate (27).

The gradient (27) is used in the update law

$$\theta(k+1) = \theta(k) - \eta(k)\frac{\partial J(k)}{\partial \theta(k)}, \quad (28)$$

where $\eta(k)$ is the *adaptive step size* given by

$$\eta(k) = \frac{1}{p_c\|B_{zu}\|_{\mathrm{F}}^2\|\Phi_{uy}(k)\|_2^2}. \quad (29)$$

It is shown in[16] that the update law (28) with the step size (29) brings $\theta(k)$ closer to the minimizer of $J(k)$ at each successive time step. Note that

implemention of the algorithm (27), (28), (29), requires that we need only know the secondary feedback matrix B_{zu} apart from the measurements z and y. The matrix B_{zu} can be obtained on-line using the time domain identification technique discussed in[20] by driving the actuators with a known broadband signal and measuring $z(k)$. An estimate $\widehat{W}_{zu}(k)$ is obtained, and an estimate $\widehat{B}_{zu}(k)$ of B_{zu} is extracted from $\widehat{W}_{zu}(k)$ and passed on to the adaptive control algorithm for the $\theta(k)$ gradient update (28). Thus, in the implementation algorithm, B_{zu} in equations (27) - (29) is replaced by an estimate $\widehat{B}_{zu}(k)$ obtained in an initialization step.

EXPERIMENTAL RESULTS

The ARMARKOV adaptive disturbance rejection algorithm described in the previous section was implemented on the experimental testbed. By measuring laser beam deflections, the optical sensor measures the membrane slope along two orthogonal axes in the plane of the membrane. The beam displacement along one axis is used as the feedback measurement $y(k)$ while the beam displacement along the axis perpendicular to it is used as the performance measurement $z(k)$. These measurements are filtered through an analog 4-pole low-pass filter with a 3 dB roll-off at 175 Hz.

The control signal generated by the disturbance rejection algorithm is used to drive the center control speaker. To initialize the algorithm, the matrix B_{zu} is identified by driving the control speaker with bandlimited white noise. The algorithm was run with $n = 28$, $\mu = 110$, $n_c = 28$ and $\mu_c = 110$ at a sampling rate of 500 Hz on a dSPACE DS1103 real-time control board. Three tests were run; two of them with single-tone disturbances at 115 Hz and 145 Hz, and one with a dual-tone disturbance at 115 Hz and 145 Hz.

Figures 6 and 7 show that almost 40 dB attenuation was obtained at the disturbance frequency for the single-tone tests. For the dual-tone disturbance, Figure 8 shows about 20 dB of attenuation at 115 Hz and 10 dB of attenuation at 145 Hz. Figure 9 shows the transient response of $z(k)$ for the single-tone disturbance at 115 Hz when the controller is turned on after approximately 1.5 seconds. None of the disturbance frequencies are known to the control algorithm.

These control experiments used only the center control speaker due to the computational burdens

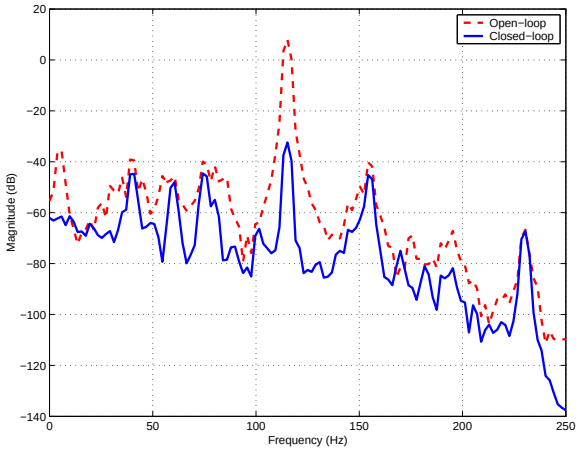

Figure 6: PSD of $z(k)$ with single-tone disturbance at 115 Hz. Closed-loop control causes 40 dB attenuation at 115 Hz.

associated with the large values of μ and μ_c. The large values were required perhaps due to the number of modes of the system or the number of zeros in the system. The drumhead has an open-loop damping of approximately 4%.

CONCLUSIONS

In this paper, we described an active vibration control testbed based on a flexible membrane using acoustic actuation, optical sensing and an adaptive disturbance rejection algorithm. Displacement attenuation of approximately 40 dB for a single-tone disturbance was obtained. The experiment was set up using the drumhead of a commercially available bass drum along with commercial audio speakers and amplifiers. The adaptive disturbance rejection algorithm proved effective for both single-tone and dual-tone disturbances, and required no knowledge of the spectrum of the disturbance and minimal knowledge of dynamics of the system. The results show an effective approach to active vibration control of flexible membranes.

ACKNOWLEDGEMENTS

We wish to thank Mark Fiebig for designing the speaker matrix and Chris Chartier for fabricating it.

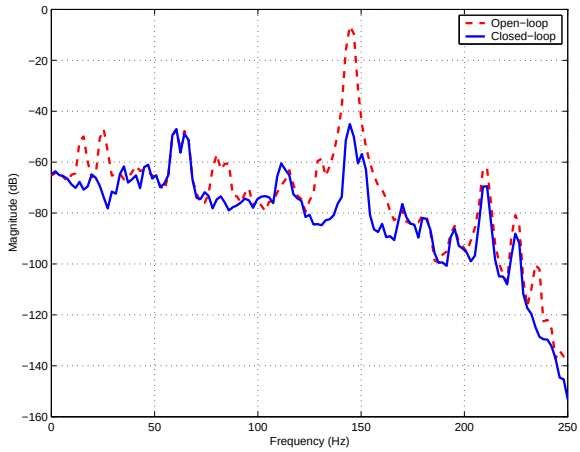

Figure 7: PSD of $z(k)$ with single-tone disturbance at 145 Hz. Closed-loop control causes 40 dB attenuation at 145 Hz.

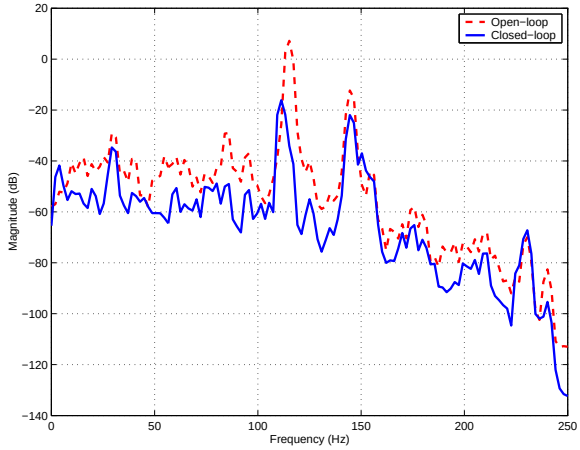

Figure 8: PSD of $z(k)$ with dual-tone disturbance at 115 Hz and 145 Hz. Closed-loop control causes 20 dB attenuation at 115 Hz and 10 dB attenuation at 145 Hz.

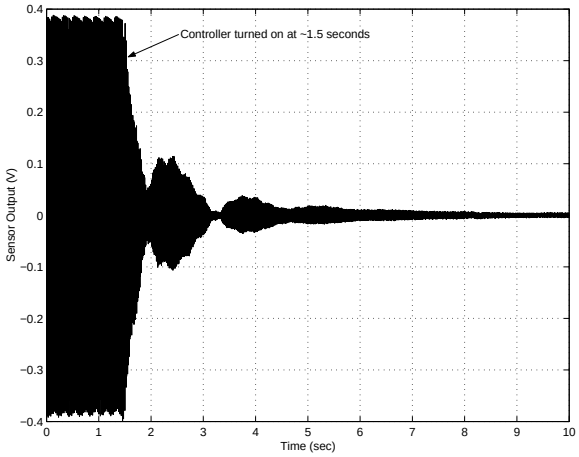

Figure 9: Time trace of $z(k)$ with single-tone disturbance at 115 Hz.

REFERENCES

[1] C. H. M. Jenkins, editor, *Gossamer Spacecraft: Membrane and Inflatable Structures Technology for Space Applications*, AIAA, Reston, VA, 2001.

[2] D. K. Marker, J. M. Wilkes, R. A. Carreras, J. R. Rotge, C. H. Jenkins, and J. T. Ash, "Fundamentals of Membrane Optics," in *Gossamer Spacecraft: Membrane and Inflatable Structures Technology for Space Applications*, AIAA, Reston, VA, 2001.

[3] R. S. Erwin, K. Schrader, R. L. Moser, and S. F. Griffin, "Experimental Demonstration of Precision Control of a Deployable Optics Structure," *J. Vibr. Acoustics*, Vol. 124, pp. 441-450, 2002.

[4] J. R. Rotge, D. K. Marker, R. A. Carreras, J. M. Wilkes, and D. Duneman, "Large Optically Flat Membrane Mirrors," Proc. SPIE, 1999.

[5] D. K. Marker, J. R. Rotge, R. A. Carreras, D. Duneman, and J. M. Wilkes, and "Minimum Strain Requirements for Optical Membranes," Proc. SPIE, 1999.

[6] M. T. Gruneisen, T. Martinez, and D. L. Lubin, "Dynamic Holography for High-Dynamic-Range Two-Dimensional Laser Wavefront Control," *Proc. SPIE*, Vol. 4493, 2002.

[7] R. A. Carreras, D. K. Marker, J. R. Rotge, J. M. Wilkes, and D. Duneman, "Deployable

Near-Net Shape Membrane Optics," *Int. Symp. Opt. Science, Eng. and Instrumentation, Proc. SPIE*, 1999.

[8] J. Hong and D. S. Bernstein, "Bode Integral Constraints, Colocation, and Spillover in Active Noise and Vibration Control," *IEEE Trans. Contr. Sys. Tech.*, Vol. 6, pp. 111-120, 1998.

[9] D. J. Mihora and P. J. Redmond, "Electrostatically Formed Antennas," *J. Spacecraft*, Vol. 17, 465-475, 1980.

[10] J. H. Lang and D. H. Staelin, "Electrostatically Figured Reflecting Membrane Antennas for Satellites," *IEEE Trans. Autom. Contr.*, Vol. 27, 666-670, 1982.

[11] J. W. Martin, J. A. Main, G. C. Nelson, J. Sirkis, and G. Washington, "Control of Deployable Membrane Mirrors," *ASME International Mechanical Engineering Congress and Exposition*, Nov. 1998, Anaheim, CA, pp. 217-223, 1998.

[12] C. H. Jenkins, D. K. Marker, and J. M. Wilkes, "Improved Surface Accuracy of Precision Membrane Reflectors through Adaptive Rim Control," *Adaptive Structures Forum*, Long Beach, CA, paper 98-1983, 1998.

[13] J. Hong, I. A. Cummings, D. S. Bernstein, and P. D. Washabaugh, "Stabilization of an Electromagnetically Controlled Oscillator," *Proc. Amer. Contr. Conf.*, pp. 2775-2779, Philadelphia, PA, June 1998.

[14] H. Sane and D. S. Bernstein, "Asymptotic Disturbance Rejection for Hammerstein Systems with Passive Linear Dynamics," *Proc. Amer. Contr. Conf.*, pp. 1449-1454, Arlington, VA, June 2001.

[15] H. S. Sane and D. S. Bernstein, "Robust Nonlinear Control of the Electromagnetically Controlled Oscillator," *Proc. Amer. Contr. Conf.*, pp. 809-814, Anchorage, AK, May 2002.

[16] R. Venugopal and D. S. Bernstein, "Adaptive Disturbance Rejection Using ARMARKOV System Representations," *IEEE Trans. Contr. Sys. Tech.*, Vol. 8, pp. 257-269, 2000.

[17] H. Sane, R. Venugopal, and D. S. Bernstein, "Disturbance Rejection Using Self-Tuning ARMARKOV Adaptive Control with Simultaneous Identification," *IEEE Trans. Contr. Sys. Tech.*, Vol. 19, pp. 101-106, 2001.

[18] R. Venugopal and D. S. Bernstein, *United States Patent 6,208,739 Noise and Vibration Suppression Method and System*, March 27, 2001.

[19] L. E. Kinsler, A.R. Frey, A.B. Coppens, and J.V. Sanders, *Fundamentals of Acoustics*, John Wiley & Sons, New York, NY, 1982.

[20] J. C. Akers and D. S. Bernstein, "Time-Domain Identification Using ARMARKOV/Toeplitz Models," *Proc. Amer. Contr. Conf.*, pp. 191-195, Albuquerque, NM, June 1997.